

Water Vapor in AGB Stars *

By

Mikako MATSUURA^{‡§}, Issei YAMAMURA^{‡¶}, Hiroshi MURAKAMI[‡] and Takashi ONAKA[§]

(November 1, 2000)

Abstract: Structure of the extended atmosphere in AGB stars has been investigated by analyzing H₂O bands in the near-infrared region. Based on simple model analysis, we concluded that the time variation in the H₂O bands with the variability phase can be attributed to the variation in the physical structure of the extended atmosphere, possibly caused by the shocks in the inner region. High wavelength/spatial resolution observations are crucial for further investigation of the structure.

1. INTRODUCTION

Asymptotic Giant Branch (AGB) stars are in the late stage of the stellar evolution for low- and intermediate-mass stars. One of the characteristics of these stars is the presence of the atmosphere which is more extended than predictions by hydrostatic models. The extended atmosphere is enriched by molecules such as CO, SiO, H₂O, and CO₂ for oxygen-rich stars, and C₂H₂ and HCN in carbon-rich stars. Dust grains are formed in the outermost region of the extended atmosphere. The matter is accelerated by the radiation pressure on the dust grains, and mass loss occurs. Most of the AGB stars are pulsating variables. The extended atmosphere has been suggested to be formed by strong pulsations in Mira variables (e.g. Bowen 1988; Fleischer, Gauger & Sedlmayr 1992; Bessell et al. 1996; Höfner et al. 1998), while the formation mechanism for weak pulsators, such as irregular variables and semi-regular variables, is still under discussion (Tsuji et al. 1997; Aoki 1999).

H₂O is one of the most abundant molecules in the atmosphere of oxygen-rich AGB stars, and is a dominant absorber in the near-infrared (near-IR) region. However, large attenuation by the terrestrial H₂O molecules hampers detailed studies of water vapor in astronomical objects from

* Based on observations with ISO, an ESA project with instruments funded by ESA Member States (especially the PI countries: France, Germany, the Netherlands and the United Kingdom) with the participation of ISAS and NASA. The SWS is a joint project of SRON and MPE.

‡ Institute of Space and Astronautical Science (ISAS), Yoshino-dai 3-1-1, Sagami-hara, Kanagawa, 229-8510, Japan; mikako@ir.isas.ac.jp

§ Department of Astronomy, School of Science, University of Tokyo, Hongo 7-3-1, Bunkyo, Tokyo, 113-0033, Japan

¶ Astronomical Institute 'Anton Pannekoek', University of Amsterdam, Kruislaan 403, 1098 SJ, Amsterdam, the Netherlands

ground-based observations. Observations from space-borne facilities are crucially needed (e.g. Neufeld et al. 1999; Truong-Bach et al. 1999; Wright et al. 2000). With the InfraRed Telescope in Space (IRTS) (Murakami et al. 1996) and the Infrared Space Observatory (ISO) (Kessler et al. 1996), several studies about H₂O lines in the oxygen-rich AGB stars have been performed. In this paper, we study the extended atmosphere of AGB stars by using the near-infrared H₂O bands and discuss the implications for future space missions.

2. THE RESULTS OF THE INFRARED TELESCOPE IN SPACE (IRTS)

The InfraRed Telescope in Space (IRTS) was launched in March 1995 and surveyed about 7% of the sky with four instruments during its 26 day mission. Two of the instruments, the Near-Infrared Spectrometer (NIRS) and the Mid-Infrared Spectrometer (MIRS), performed spectroscopic observations. The NIRS covers the wavelength from 1.43 to 2.54 and from 2.88 to 3.98 μm in 24 channels with a spectral resolution for point sources of $\Delta\lambda = 0.10\text{--}0.12 \mu\text{m}$. The MIRS covers the range from 4.5 to 11.7 μm in 32 channels with a resolution of $\Delta\lambda = 0.23\text{--}0.36 \mu\text{m}$. Both spectrometers have a rectangular entrance aperture of $8' \times 8'$. Total numbers of detected point sources are about 50,000 for the NIRS (Freund et al. 1997) and about 1,000 for the MIRS (Yamamura et al. 1996). The results of the IRTS about water vapor bands were reported in Matsuura et al. (1999). Figure 1 shows the representative spectra of oxygen-rich stars obtained by the IRTS. Matsuura et al. (1999) selected 108 bright stars in high galactic region, and found water vapor features in 6 early M-type giants. The presence of H₂O in these early M-type giants has not been predicted by hydrostatic models. Column densities and excitation temperatures of the water vapor were estimated in two of these early M-type stars by model fitting. Figure 2 shows the water vapor spectrum in AK Cap compared with the synthesized spectra. From the fitting, the excitation temperature between 1000 K and 1500 K and the column density of $5 \times 10^{19} \text{ cm}^{-2}$ are derived. The relatively low excitation temperature suggests that the observed H₂O molecules are located in the extended atmosphere, and not in the photosphere. The water molecules revealed the presence of the extended atmosphere even in these early M-type stars.

3. THE RESULTS OF THE INFRARED SPACE OBSERVATORY (ISO)

Using ISO/SWS (Short-Wavelength Spectrometer) (de Graauw et al. 1996), Tsuji et al. (1997) reported the detections of the molecular features such as H₂O, CO₂ and SiO, arising from the extended atmosphere. The excitation temperatures range between 750–2000 K. The effective radii of these molecules are about 2 stellar radii. As the abundance ratio of these molecules is inconsistent with the one predicted from thermochemical equilibrium, the authors suggested that non-equilibrium chemistry must be important in this region.

Yamamura, de Jong, & Cami (1999) found that the water vapor bands are seen in emission around 3.8 μm in *o* Cet, which was observed at maximum in the visual light curve. In contrast, Z Cas, which was observed at minimum, showed absorption features at the same wavelengths. They analyzed water vapor bands from 2.5 to 4.0 μm with a simple ‘slab’ model, consisting of two molecular layers (‘hot’ layer and ‘cool’ layer) with independent excitation temperatures (T_H , T_C), column densities (N_H , N_C), and radii (R_H , R_C). Plane-parallel configuration and local thermodynamic equilibrium (LTE) were assumed for simplification. Stellar continuum was assumed to be a 3000 K black body. The most interesting results are the difference in the radius of the ‘hot’ layer (R_H) in the two stars. The radius of the ‘hot’ layer with an

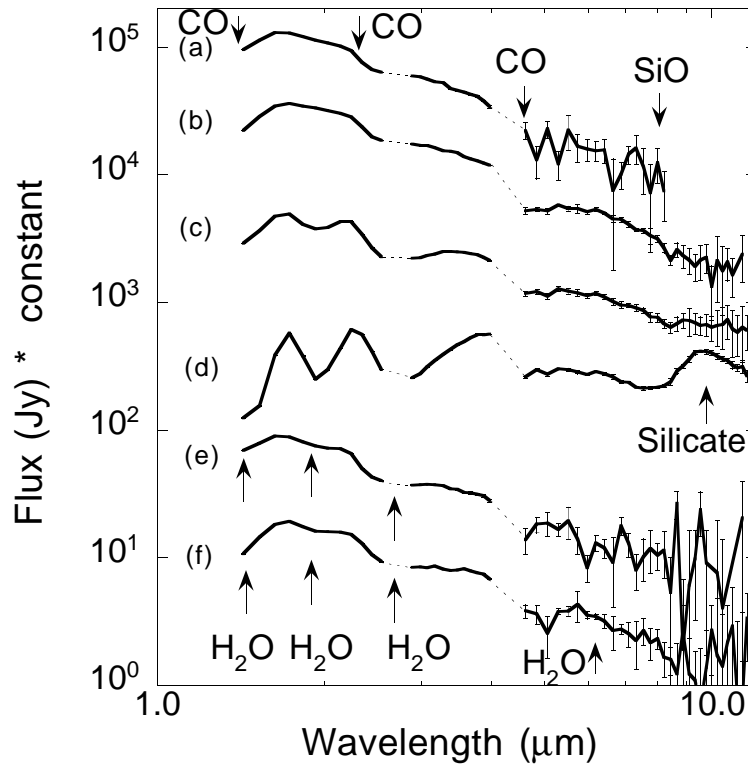


Fig. 1: The combined NIRS & MIRS spectra of M-giants are shown. From top to bottom: (a) HR 1667 (M2III), (b) HR 257 (M4III) (c) X Hor (M6-M8, SRa), (d) RR Aql (M6e-M9, Mira), (e) AK Cap (M2, Lb), and (f) V Hor (M5III, SRb). Water absorption bands at 1.9 and 2.7 μm are seen in two early M-giants (e) AK Cap and (f) V Hor, in contrast to other early M-giants ((a) and (b)). This figure is taken from Matsuura et al. (1999).

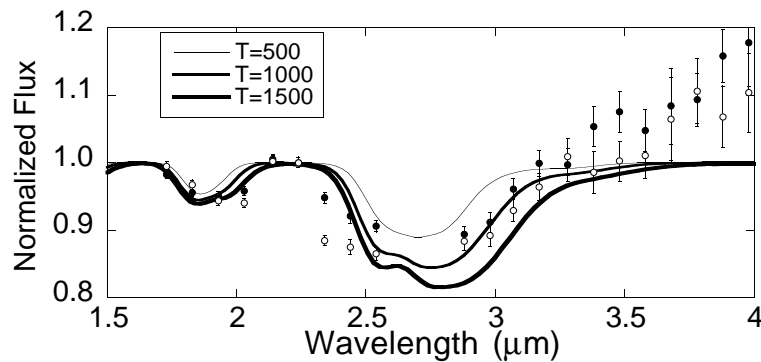


Fig. 2: The observed spectral profile of H_2O in AK Cap (M2), divided by the spectra of HR 1667 (M2; open circle) and HR 6306 (M2; filled circle), and normalized at 2.2 μm . Both HR 1667 and HR 6306 indicate neither H_2O bands nor dust emission. The three lines show LTE model spectra with a column density of $5 \times 10^{19} \text{ cm}^{-2}$, and excitation temperatures of 500, 1000, and 1500 K. The excess at longer wavelength in the observation is possibly due to dust emission. This figure is taken from Matsuura et al. (1999).

excitation temperature of 2000 K influences the features longer than $\sim 3.5 \mu\text{m}$. This is clearly demonstrated by a sharp peak at $3.83 \mu\text{m}$ in Figure 3. Yamamura, de Jong, & Cami (1999) indicated that the ‘hot’ layer extends to $\sim 2 R_*$ in *o* Cet and to $\sim 1 R_*$ in Z Cas, where R_* is the radius of the background stellar continuum. They suggested that the ‘hot’ water layer is more extended at maximum phase than at minimum, and makes the difference in the features.

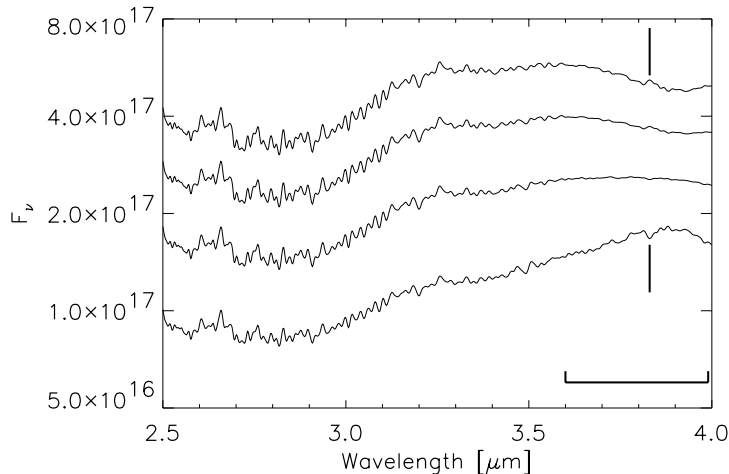


Fig. 3: The effects of R_H on the synthesized spectra are shown. From top to bottom, R_H is 2.2, 1.8, 1.4, 1.0 R_* . The features longer than $\sim 3.5 \mu\text{m}$ vary with R_H . Features become emission when R_H is larger than $\sim 1.5 R_*$. The absolute flux changes due to the variation of radius of the emitting region. Other parameters are fixed as $T_H = 2000 \text{ K}$, $T_C = 1200 \text{ K}$, $N_H = 1 \times 10^{22} \text{ cm}^{-2}$, $N_C = 1 \times 10^{21} \text{ cm}^{-2}$. In these calculations, R_C is given as $R_C^2 = R_H^2 + 1^2 [R_*^2]$.

Matsuura et al. (in preparation) further examine the time variation in the H_2O bands in the $2.5\text{--}4.0 \mu\text{m}$ region. The spectra at different variability phases were obtained by the ISO/SWS for four Mira variables over longer than one variable cycle (Onaka et al. 1999; Loidl et al. 1999). Figure 4 shows an example of the time variation of the observed spectra, and Figure 5 indicates the corresponding synthesized spectra by the model in Yamamura, de Jong, & Cami (1999). Only H_2O molecules are included in the model. The time variation of the H_2O bands should be attributed to the variation in the excitation temperature, the column density, and the radius. Figure 6 shows the variation in the radius of ‘hot’ layer with the visual phases. The radius of the ‘hot’ layer reaches more than $2 R_*$ around maximum ($\phi=0.0, 1.0, \& 2.0$) and becomes $\sim 1 R_*$ around minimum. As the radius of the stars at the continuum wavelengths is rather stable compared to the variation scale of the ‘hot’ layer (Tuthill, Haniff, & Baldwin 1999), these results indicate that the time variation of the infrared water bands is mainly caused by the variation in the physical structure of the extended atmosphere and the location of the H_2O emitting region. Hinkle & Barnes (1979) measured the radial velocity of H_2O lines in the Mira variable, R Leo. They suggested that the warm H_2O molecules with an excitation temperature of $\approx 1700 \text{ K}$ are located near the boundary of the photosphere. The radial velocity of the warm H_2O component varies linearly from -2 to 30 km s^{-1} during the phase of $\phi=0.0\text{--}1.0$ (Hinkle & Barnes 1979). The systemic velocity of R Leo is 8 km s^{-1} (Hinkle 1978). If one assumes that the velocity of the warm H_2O molecules with respect to the systemic velocity probes the motion

of that layer, one could obtain the location of the H_2O layer at a certain phase by integrating the velocity. The estimated scale of the H_2O displacement over a half period is roughly $0.3 R_*$ ($3 \times 10^{13} \text{ cm}^{-2}$ is adopted for $1 R_*$), and is smaller than the variation in R_H . Thus, the variation in the H_2O emitting region is probably attributed to the variation in the temperature structure in the extended atmosphere. Shocks caused by the pulsation penetrate into the expanded atmosphere. They could heat up the molecules locally. They could also destroy the molecules, and changes the radial distribution of the molecular density. These variations of the physical structure in the extended atmosphere possibly leads to the time variation of the H_2O bands.

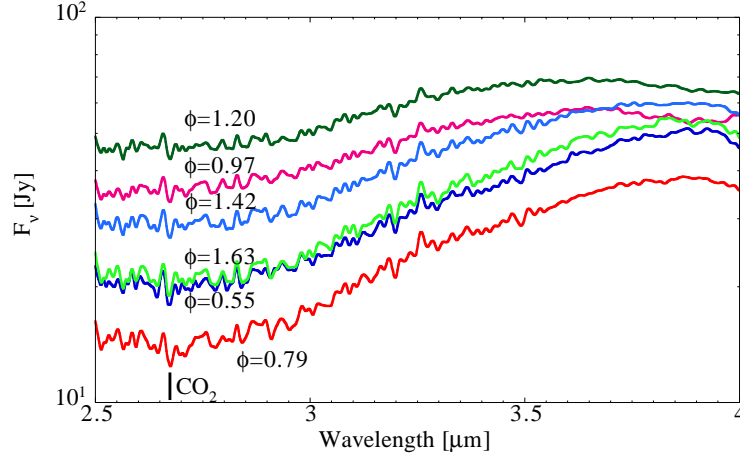


Fig. 4: The time variation in the spectra of Z Cyg obtained by ISO/SWS. The optical phase at each observation determined by the AAVSO light curve, is denoted in the figure. A sharp absorption at $2.68 \mu\text{m}$ is due to CO_2 .

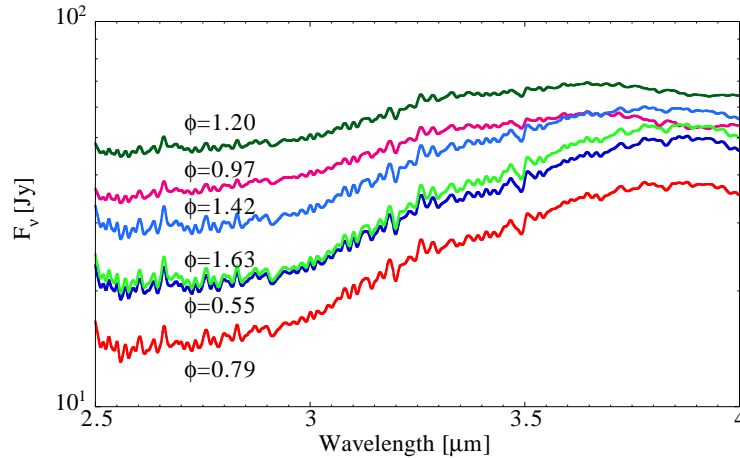


Fig. 5: The synthesized spectra corresponding to Figure 4 are indicated. Global shape and most of the features in this wavelength region are reproduced by the model including only H_2O .

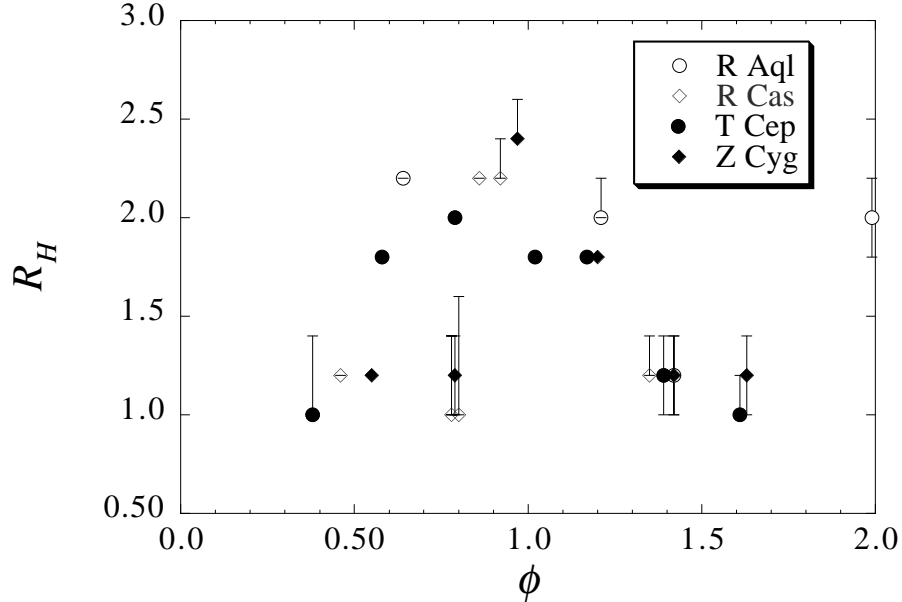


Fig. 6: Preliminary results of derived R_H are indicated. The radius of hot layer is about $\sim 1 R_*$ around minimum, and about $\sim 2 R_*$ around maximum. Note that in the current analysis, the excitation temperature of the hot layer is fixed as 2000 K. When the excitation temperature of the hot layer is a free parameter, the radius of the hot layer might be affected. The effect is approximately $0.2 R_*$.

4. IMPLICATIONS FOR THE FUTURE SPACE MISSIONS

Observations of the polyatomic molecules, such as H_2O , CO_2 , SO_2 , demonstrate the complicated structure of the extended atmosphere (Yamamura et al. 1999; Yamamura, de Jong, & Cami 1999; Woitke et al. 1999; Cami et al. 2000; Matsuura et al. in preparation; Yamamura 2000). Due to the interferences by terrestrial molecules, studies of these polyatomic molecules require spectroscopic observations from space-born facilities. Among the polyatomic molecules, H_2O is the most abundant molecule in oxygen-rich environment, and is detected in many AGB stars, even in early M-type stars. Thus, H_2O enables us detailed studies of the extended atmosphere in AGB stars. H_2O molecule has a number of transitions in the infrared region and they come from various regions not only in the extended atmosphere but also in the circumstellar envelope. Thus, observations with a wide wavelength-coverage will lead to a comprehensive view of the structure in the outer regions of the stellar atmosphere.

Here we list the implications for the future space missions.

- High resolution spectroscopic observations especially in the near- and mid-infrared regions are required to examine the dynamical motion of the extended atmosphere (required resolution: $< 3 \text{ km s}^{-1}$). High-spatial-resolution observations are also desirable.
- AGB stars are long period variables with a period of about 1 year or longer. The time-scale of the variation in the spectra, or the variation in the structure in the extended atmosphere, is longer than 1 period. Periodical monitoring over more than 1 period with a stable instrument is necessary. Long mission lives (longer than 3 years) are required.

ACKNOWLEDGMENT

The authors acknowledge Drs. M. Cohen and M. Noda for their efforts on the NIRS calibration, and Drs. M. M. Freund and M. Tanaka for the NIRS-data reduction. We acknowledge AAVSO International Database to provide light curve of R Aql, R Cas, T Cep and Z Cyg. M. M. thanks people at the University of Amsterdam, especially Profs. de Jong and Waters, for the discussions and the hospitality during her stay. M. M. is supported the Research Fellowships of the Japan Society for the Promotion of Science for Young Scientists.

REFERENCES

- Aoki, W., 1999, PhD thesis, University of Tokyo
Bessell, M. S., Scholz, M., & Wood, P. R. 1996, *A&A*, 307, 481
Bowen, G. H. 1988, *ApJ*, 329, 299
Cami, J. et al. 2000, *A&A*, 360, 562
de Graauw, Th. et al. 1996, *A&A*, 315, L49
Fleischer, A. J., Gauger, A., & Sedlmayr, E. 1992, *A&A*, 266, 321
Freund, M. M. et al. 1997, in: ASP Conf. Ser. 124, *Diffuse Infrared Radiation and the IRTS*, ed. H. Okuda, T. Matsumoto, & T. L. Roellig (San Francisco: ASP), 67
Hinkle, K. H. 1978, *ApJ*, 220, 210
Hinkle, K. H. & Barnes, T. G. 1979, *ApJ*, 227, 923
Höfner, S. et al. 1998, *A&A*, 340, 497
Kessler, M. et al. 1996, *A&A*, 315, L27
Loidl, R. et al. 1999, *ESASP*, 427, 365
Matsuura, M. et al. 1999, *A&A*, 348, 579
Murakami, H. et al. 1996, *PASJ*, 48, L41
Neufeld, D. A. et al. 1999, *ApJ*, 517, L147
Onaka, T. et al. 1999, *ESASP*, 427, 281
Tsuji, T. et al. 1997, *A&A*, 320, L1
Truong-Bach et al. 1999, *A&A*, 345, 925
Tuthill, P. G., Haniff, C. A., & Baldwin, J. E. 1999, *MNRAS*, 306, 353
Woitke, P. et al. 1999, *A&A*, 348, L17
Wright, C.M. et al. 2000, *A&A*, 358, 689
Yamamura, I. et al. 1996, *PASJ*, 48, L65
Yamamura, I. et al. 1999, *A&A*, 341, L9
Yamamura, I., de Jong, T., & Cami, J. 1999 *A&A*, 348, L55
Yamamura, I. 2000, this volume